We are IntechOpen, the world's leading publisher of Open Access books Built by scientists, for scientists

4,800
Open access books available

122,000
International authors and editors

135M
Downloads

Our authors are among the

154
Countries delivered to

TOP 1%
most cited scientists

12.2%
Contributors from top 500 universities

CLARIVATE ANALYTICS BOOK CITATION INDEX INDEXED

WEB OF SCIENCE™

Selection of our books indexed in the Book Citation Index in Web of Science™ Core Collection (BKCI)

Interested in publishing with us?
Contact book.department@intechopen.com

Numbers displayed above are based on latest data collected.
For more information visit www.intechopen.com

Chapter 7

Energy Transfer in Graphene-Based Hybrid Photosynthetic Nanostructures

Sebastian Mackowski and Izabela Kamińska

Additional information is available at the end of the chapter

http://dx.doi.org/10.5772/64300

Abstract

Energy transfer is one of the most fundamental processes at the nanoscale. Whenever a donor is placed sufficiently close to an acceptor, they could couple via electrostatic interactions and the energy is funnelled down to the acceptor. Only recently graphene, a two-dimensional sp2-hybridized carbon hexagonal lattice, has emerged as highly attractive from the point of view of potential applications in photonics and optoelectronics, as it features uniform absorption, which extends over the whole visible range down to the infrared. With the absence of fluorescence, it renders graphene as an exceptional acceptor in devices that utilize energy and/or electron transfer. In this chapter, we review recent work on the energy transfer in graphene-based assemblies involving also graphene derivatives (graphene oxide and reduced graphene oxide), as well as describe results of fluorescence studies focused on interactions between graphene and photosynthetic protein—pigment complexes. While for organic dyes the efficiency of the energy transfer is very high, in the case of the proteins, there is some shielding of chlorophylls from graphene, partially inhibiting the energy transfer. This allows for observing interesting effects associated with dependencies on the excitation energy, number of graphene layers, or the substrate that graphene is placed onto.

Keywords: graphene, reduced graphene oxide, photosynthetic complex, energy transfer, fluorescence microscopy, fluorescence imaging

1. Introduction

Non-radiative energy transfer (ET) is one of the most fundamental processes at the nanoscale. It is associated with funnelling excitation energy between molecules, quantum dots or other nanostructures [1]—in most cases—via dipole-dipole interaction. Such a scheme evolved

for instance in natural photosynthesis [2] for efficient capturing and transport of the sunlight energy, and has been recently implemented in artificial light-harvesting assemblies [3]. The efficiency of ET depends on the spectral properties of a donor and an acceptor, their mutual orientation, as well as separation between them [4]. In particular, the distance dependence of the ET efficiency, which for localized dipoles scales with d^{-6}, has been exploited as a useful tool to measure lengths at the nanoscale, both statically and dynamically. In particular, the energy transfer has been considered an attractive way to control light harvesting and bio(sensing) [5–7]. As a result, various strategies had to be devised to fabricate hybrid nanostructures with well-defined morphology required for controlling the energy transfer efficiency. Among the most feasible, one can find robust nanolayers, either polymer or dielectric, deposited on a surface of nanoparticles or a substrate [8, 9], and more flexible linkers based for instance on DNA strands or biotin-streptavidin conjugation [10, 11].

Another critical parameter that influences the interaction between two dipole moments in the context of the energy transfer is the relation of their spectral properties. Namely, as shown in **Figure 1**, the absorption of one of the molecules (acceptor) has to overlap with the emission of the second molecule (donor). The larger the overlap, the higher the efficiency of the energy transfer. The final parameter that has to be considered in energy transfer geometry is the mutual orientation of the dipole moments of a donor and an acceptor. All these factors are included in the equation shown in **Figure 1**. It is important to note that the equation describes the case where both donors and acceptors are classical dipole moments.

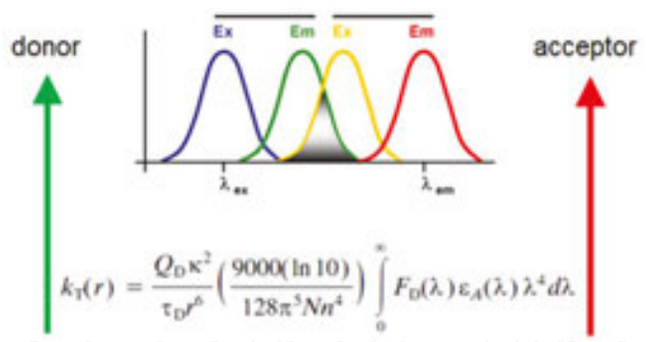

Figure 1. Schematic representation of the energy transfer between two dipole moments of a donor (green) and acceptor (red). The energy transfer is possible only when the emission of the donor overlaps with the absorption of the acceptor.

Optical spectroscopy, and in particular fluorescence spectroscopy, provides a variety of tools to probe the energy transfer in hybrid nanostructures. It stems from the fact that the emergence energy transfer results in the decrease of the emission intensity of a donor at the expense emission intensity of an acceptor. This is in fact the most straightforward consequence energy transfer between two nanostructures. In addition to the intensity flow between donors and acceptors, another signature of the energy transfer is a shortening of the fluorescence decay time of the donor. Indeed, the energy transfer can be considered as a new channel for nonradiative recombination from the point of view of the donor, and as such it should result in shortening of the lifetime.

http://dx.doi.org/10.5772/64300

The purpose of this chapter is to review recent research carried out on hybrid nanostructures composed of graphene and graphene derivatives and naturally evolved photosynthetic complexes. Our aim is to emphasize effects that are not readily available when studying classical emitters, such as organic dyes or semiconductor nanocrystals, which have spectrally limited absorption and emission, as in contrast to these, photosynthetic complexes feature absorption that spans over the whole visible spectral range. They are also pigment-protein complexes, with chlorophyll molecules protected from the environment. Thus, the interaction between photosynthetic complexes and graphene is not immediate. However, before we describe the results obtained for photosynthetic complexes coupled with graphene, we review several key results reported for organic dyes and semiconductor nanocrystals on graphene. This is important to illustrate basic mechanisms and processes that take part in such hybrid architectures.

2. Overview of recent results

2.1. Graphene: basic properties

Graphene is nowadays one of the most intensively studied materials. Since 2004, when it was for the first time obtained by mechanical exfoliation, many research groups worldwide have focused on understanding and proving uniqueness of this one-atom thin material [12, 13]. Part of these efforts were inspired by the combination of properties rarely met in any other material, such as exceptionally high electronic and thermal conductivity, mechanical strength, unusual electronic structure and optical transmittance, impermeability to gases and many others [14].

The key property of graphene, which impacts its electronic and optical character, and is particularly important in the context of light-matter interactions, is an unusual zero bandgap structure and linear dispersion near the Brillouin zone corners. Indeed, in the case of graphene, the conduction and valence bands meet at Dirac points and in their vicinity the energy depends linearly on the wavevector [15]. Consequently, both electrons and holes mimic massless relativistic particles with effective velocity of $c^* \approx 1/300$ the speed of light.

Fully occupied valence band combined with an empty conduction band, and no energy gap between them, leads to unique electronic absorption of graphene. Remarkably, it is rather high, and for a suspended graphene monolayer is defined solely by the fine-structure constant, which translates to 2.3% absorption of incident light (**Figure 2**) [16]. In addition, the absorption of graphene shows no wavelength dependence from ultraviolet to near-infrared. Therefore, graphene sheets can be visualized using optical microscopy, as shown in **Figure 2**, and the absorption of a few-layer graphene can be roughly described as a sum of non-interacting single layers with each layer contributing 2.3% of opacity. From the point of view of hybrid assemblies where the energy transfer is exploited, graphene can be utilized as energy acceptor due to uniform absorption, but at the same time, it features no fluorescence emission. Consequently, any effects attributable to the energy transfer from any emitter to graphene will have to be probed and quantified based solely on the behaviour of energy donors.

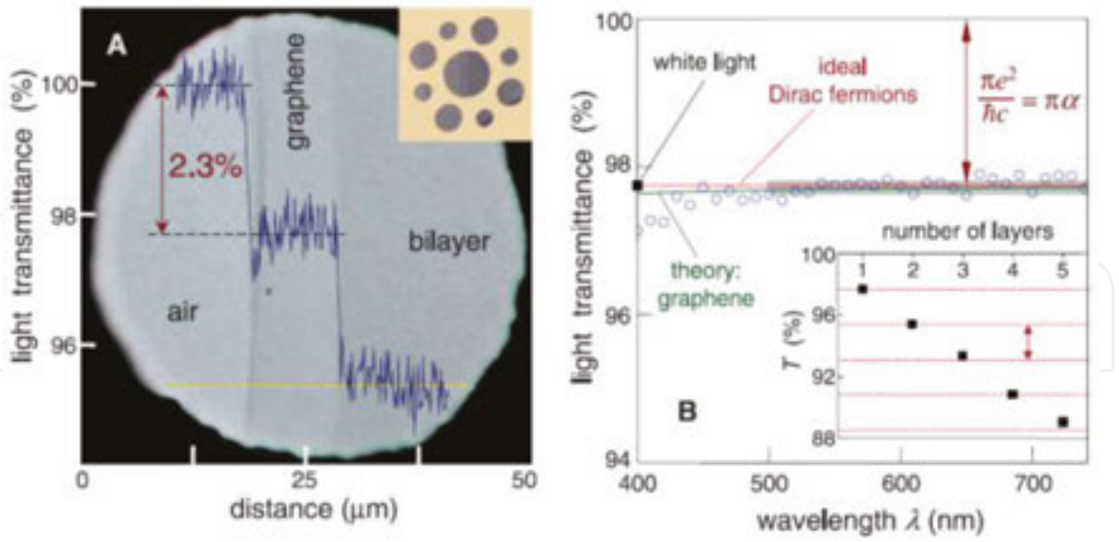

Figure 2. (A) Photograph of a 50-mm aperture partially covered by monolayer and bilayer graphene. The line-scan profile shows the intensity of transmitted white light along the yellow line. (Inset) Sample design. (B) Transmittance spectrum of single-layer graphene (open circles). The red line is the transmittance expected for two-dimensional Dirac fermions, whereas the green curve takes into account a non-linearity and triangular warping of graphene's electronic spectrum. (Inset) Transmittance of white light as a function of the number of graphene layers (squares). From Nair et al. [16]. Reprinted with permission from AAAS.

2.2. Graphene: fabrication methods

There are several ways of obtaining graphene and its derivatives, with each method holding specific advantages depending on particular application [17], but also facing limitations from the point of view of scalability, cost, reproducibility and alike.

First experiments on graphene have been carried out for the highest-quality pristine graphene obtained by mechanical exfoliation. This method, which is still arguably the leading one, allows preparing pure hexagonal carbon lattice without defects or dopants, thus exfoliated graphene has been at the centre of fundamental studies of its properties [16, 18]. It suffers, however, from small and irregular sample sizes and shapes, low throughput and high prices.

Growing demand for larger and reproducible graphene pieces has resulted in the development of other methods used for the production of two-dimensional (2D) carbon materials. Epitaxial techniques, by both sublimation and chemical vapour deposition (CVD), are the most promising due to the comparably high quality of fabricated graphene combined with high reproducibility and scalability. The first approach involves decomposition of SiC in low pressures (or ultra-high vacuum) and high temperatures. Addition of the annealing in argon atmosphere significantly improves homogeneity of graphene [19]. Upon sublimation of silicon from SiC surface, the remaining carbon atoms form graphene layers. Although the price of SiC substrate is relatively high, it could be compensated by excellent electronic parameters of graphene and performance of fabricated devices [13].

An alternative approach to produce graphene is CVD, which involves deposition of hydrocarbons onto a transition metal surface, usually copper or nickel, which works as a catalyst

http://dx.doi.org/10.5772/64300

[20, 21]. Due to the differences of solubility of carbon in Ni and Cu, the processes also differ from each other. As the solubility of carbon in Cu is rather low, the formation of graphene layers weakly depends on the actual conditions of the growth process. This allows for a better control over graphene growth, and when the monolayer is formed the deposition process stops. For this reason, large domains of single graphene layers are formed (>95% of the surface) [20]. Although graphene growth on Cu displays some disadvantages, such as wrinkles and grain boundaries, it is a relatively simple and inexpensive approach, suitable for mass production of high-quality graphene. Importantly, graphene grown on metallic surfaces can be transferred via polymer-assisted method on any arbitrary substrate, what is important for constructing graphene-based devices (photovoltaic cells, transistor, etc.) [22].

For uniform graphene layers obtained using exfoliation or CVD, hybrid assemblies for studying the energy transfer have to be constructed in a layer-by-layer geometry, where emitters are deposited onto the graphene layer (or on a polymer/oxide layer that is supposed to separate emitters from graphene).

In addition to methods that allow for growing large-area uniform graphene with well-controlled number of layers, other approaches have also been developed, based on the concept of liquid phase exfoliation. The approach of synthesizing two-dimensional carbon flakes in liquid relies on the reduction of graphene oxide (GO) [23] and key advantages thereof include solubility in aqueous and organic solvents, easy processing and surface functionalization, cheap synthesis for scalable production and relatively mild conditions of synthesis [24].

Briefly, the process usually starts with oxidizing graphite using one of the many popular oxidation methods: Hummers, Brodie or Staudenmaier [25, 26]. In the next step, due to the presence of oxygen-containing functional groups (hydroxyls, carbonyls, carboxyls or oxygen epoxides), graphite oxide can be easily exfoliated into GO via ultrasonication or mechanical stirring. Importantly, the presence of oxygen moieties distinguishes GO from graphene, and due to the predominance of sp^3- over sp^2-hybridized carbon atoms, GO is a fluorescent insulator, as opposed to graphene, which is a non-emitting conductor. However, it is an ideal precursor for the synthesis of reduced GO (rGO), also called chemical graphene. Importantly, by reducing GO, and thus restoring the sp^2-carbon network without additional components and residues [50, 51], it is possible to not only diminish fluorescence but also retrieve electrical and thermal conductivity. In contrast to graphene, rGO can be dispersed in water, and preparation of rGO flakes in solution makes it feasible to incorporate various functional groups on the surface, as required for many applications.

Among the key challenges is the establishment of reproducible methods of fabricating large-area rGO flakes and assuring the control of the number of layers, although these two factors frequently compete against each other: it is difficult to fabricate large single-layer rGO. The most commonly applied strategies are mild oxidation conditions, which promote the formation of larger flakes simply by reducing cracking of graphite flakes [27], adding a pretreatment step (an incubation in sulphuric acid with gentle stirring) before oxidation [28], or even skipping sonication to avoid breakage of flakes [29]. An important step is a separation of large flakes from aggregates and smaller sheets, and this can be performed with a high-speed centrifugation [27, 30, 31]. Also, GO might be deposited on a substrate using Langmuir-

Blodgett technique or self-assembling, before subsequent reduction, either chemically or thermally, to prevent re-aggregation of rGO flakes [29, 32].

From the point of view of the energy transfer, rGO offers important degree of freedom as compared to epitaxial graphene, namely it is possible to prepare mixtures in solution, which is often technically simpler and more suitable for—for instance—fluorescence-sensor design.

2.3. Graphene as energy acceptor

Constant absorption covering ultraviolet, visible and near infrared spectral regions (300–2500 nm), together with unusual electronic structure, renders graphene as an exceptional energy acceptor. It is possible to obtain not only energy transfer from any emitter to graphene but also the zero-energy gap of graphene implies that any interactions in graphene-based hybrid nanostructures can be investigated exclusively by studying optical properties of a donor. These properties result in a unique potential of graphene as a component of devices designed for photonics, optoelectronics, as well as photodetectors and biosensors. In particular, in recent years several studies emerged, where the energy transfer from various emitters to graphene has been investigated.

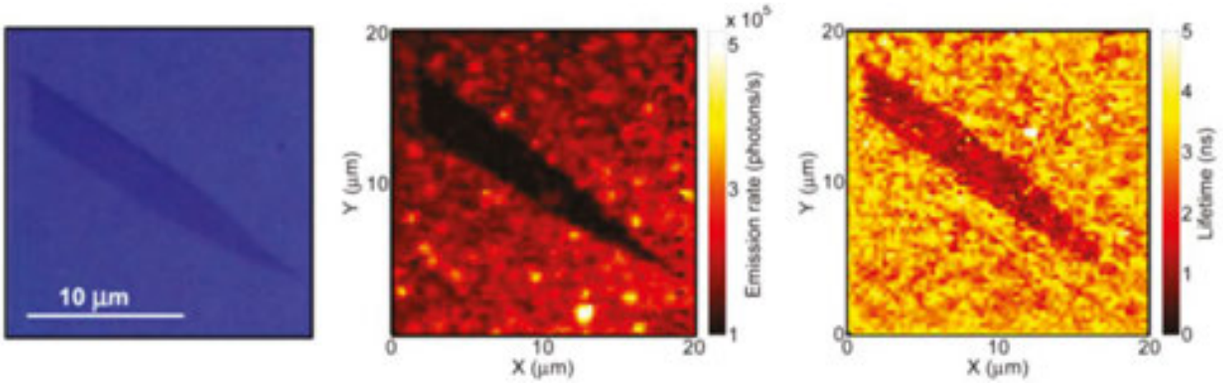

Figure 3. Images of the same area of the sample containing a monolayer graphene sheet (darker field on the left image) obtained with optical microscope, fluorescence microscope, where the emission intensity of Rhodamine dyes was measured, and fluorescence lifetime imaging microscope, where decay times of fluorescence were measured. Significant decrease of the intensity of Rhodamine on graphene is accompanied with drastic reduction of the decay time. From Gaudreau et al. [33]. Reprinted with permission from ACS.

One of the first hybrid structures where the energy transfer to graphene was investigated comprised a layer of Rhodamine molecules on a graphene flake [33], as shown in **Figure 3**. The position and shape of the graphene flake can be determined by optical microscopy and next by collecting a fluorescence image of the same area, any influence of the presence of graphene on the fluorescence properties of Rhodamine can be extracted. In this work [33], the authors included also time-resolved fluorescence lifetime-imaging microscopy. In order to study the dependence of the energy transfer on the distance between the emitters and graphene, a layer of PMMA polymer with a thickness from 5 to 20 nm was deposited on graphene. As can be seen in **Figure 3**, for molecules placed on graphene the fluorescence intensity is significantly less as compared to the reference. This decrease of emission intensi-

http://dx.doi.org/10.5772/64300

ty is accompanied with strong reduction of fluorescence lifetime. Both these spectral signatures are indication of the energy transfer from Rhodamine to graphene. Estimated maximum efficiency of the energy transfer was equal to 99% and it decreased with the spacer thickness. It was experimentally proved that the energy transfer to graphene scales with the distance as d^{-4}, which is different from the classic case of two interacting dipole moments. This difference is indicative of the universal value of the optical conductivity (assigned to gapless and 2D lossy media) and is in agreement with theoretical results obtained by Sebastian and Swathi [34]. There are two major consequences of these results: high efficiencies of the energy transfer indicate that in order to study energy transfer from a dye to graphene it might be critical to use a spacer, as otherwise fluorescence of the emitters can be totally quenched. There are, however, examples, where particular orientation of the molecules on a graphene surface partially inhibited the energy transfer [35]. Furthermore, weaker relation between the decay rate and distance can make it possible to investigate donor-acceptor interactions for distances unavailable for pairs of two classical dipoles.

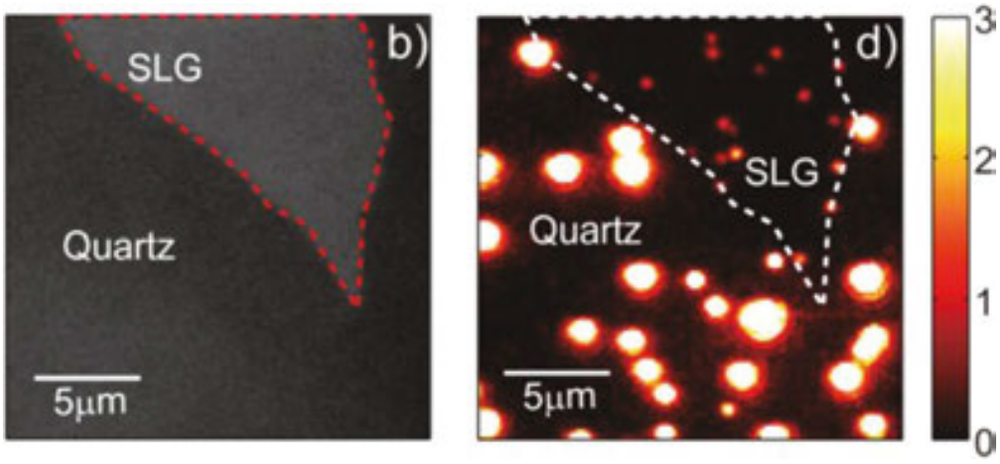

Figure 4. Optical and fluorescence images of individual nanocrystals on single-layer graphene and on the quartz substrate; (b) optical reflectivity image in the emission range of nanocrystals; (d) wide-field fluorescence image of individual CdSe-ZnS nanocrystals in the region shown in panel (b). The colour scale bar indicates the number of emitted photons (in arbitrary units) integrated over 30 s. From Chen et al. [36]. Reprinted with permission from ACS.

An important advancement into elucidating the energy transfer to graphene was experimental observation of fluorescence quenching of individual semiconductor nanocrystals [36]. For this experiment, micrometer-size sheets of graphene monolayer were used, on which highly diluted solution of CdSe/ZnS nanocrystals was deposited (**Figure 4**). By combining optical and fluorescence imaging, it was possible to correlate the differences in fluorescence intensity of individual nanocrystals with the locations where graphene was present. The result was dramatic (70-fold) quenching of fluorescence intensity for nanocrystals placed on graphene. Moreover, the quenching efficiency was found to increase with a number of graphene layers. This observation was explained using a simple model of a few-layer graphene, in which weak interactions between layers can be neglected, so the quenching factor is calculated for n layers of non-interacting single graphene planes. The significance of these results is in removing any

ensemble averaging that is always present in experiments performed on layers, as the one described above. In addition, when layers of emitters are studied, there is always a certain thickness of this layer, across which the strength of the interaction, in this case the energy transfer, varies, sometimes considerably. As a result, an average effect is measured in fluorescence microscopy experiment, similarly as in the case of plasmonic interactions associated with metallic nanoparticles [37]. In this context, the value of single nanocrystal experiment manifests itself in the observation of suppression of fluctuations of fluorescence intensity of single nanocrystals upon deposition on graphene. This indicates the effect of graphene-induced fluorescence quenching also on the photophysics of the nanocrystals.

Very recently, both concepts were combined in a single experiment, where distance dependence of the energy transfer rate to a monolayer graphene was studied for individual emitters, both zero-dimensional CdSe/CdS nanocrystals and two-dimensional CdSe/CdS/ZnS nanoplatelets [38]. Both types of energy donors were separated from graphene with ultrasmooth dielectric film of magnesium oxide with a thickness varied from just a few Å up to several tens of nanometers. In terms of radiative energy transfer efficiency (>95%), both structures exhibited similar behaviour upon direct coupling to graphene. Important differences appear when emitters are separated from graphene with a spacer. While for zero-dimensional nanocrystals the energy transfer rate scales with a distance according to d^{-4} law, the energy transfer rate of the two-dimensional platelet decays is affected to a lesser degree. This is explained by a theoretical model, which includes the contribution of thermal distribution of free excitons in a two-dimensional quantum well at finite temperatures. The results confirm that graphene-nanocrystal hybrid structure, governed by both charge transfer and Förster-type resonant energy transfer, is a suitable system to explore the influence of exciton dimensionality and localization, as well as distance, on the energy transfer rate (**Figure 5**).

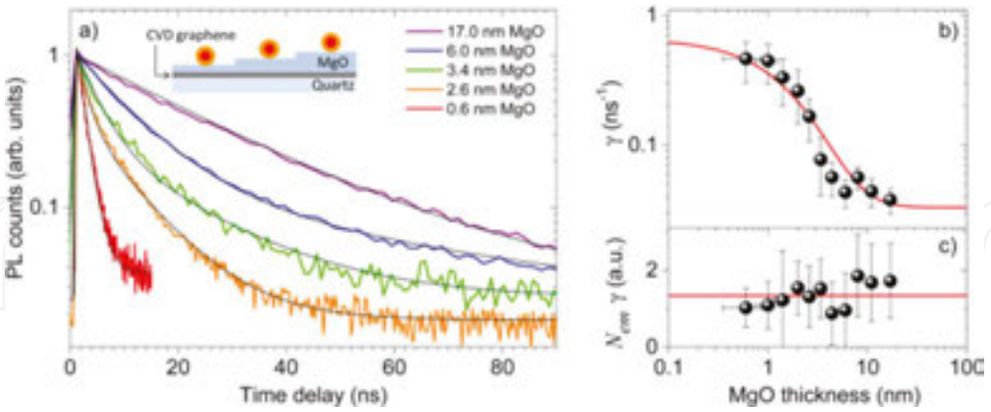

Figure 5. (a) Selected luminescence decays of individual CdSe/CdS nanocrystals separated from graphene by an MgO spacer with increasing thickness. The thin black lines are fits based on biexponential decays convoluted with the instrument response function. (b) Statistically averaged measured decay rate γ as a function of the thickness of the MgO spacer. (c) Statistically averaged product of the number of emitted photons per exciting laser pulse N_{em} and the decay rate γ. From Federspiel et al. [38]. Reprinted with permission from ACS.

Very efficient energy transfer from organic dyes to graphene-based materials has also been used to visualize the structure and determine the morphology of graphene-dye hybrids.

Fluorescence quenching microscopy is a practical tool for detecting and mapping of graphene flakes [39]. Contrary to Raman spectroscopy or optical techniques, in this case an additional component of energy donor is necessary. This is compensated by significantly increased contrast, as well as faster and more sensitive data recording of large areas compared to optical imaging (**Figure 6**) and Raman spectroscopy.

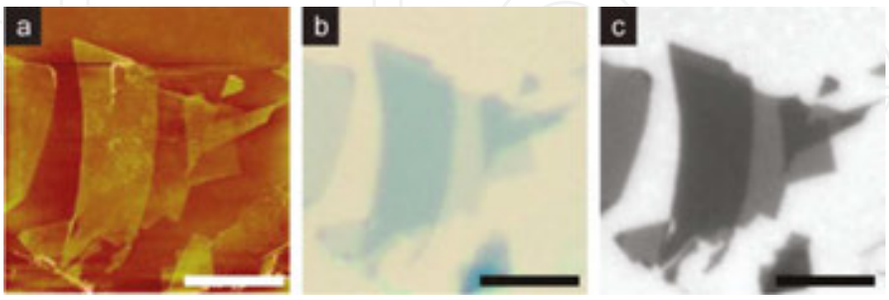

Figure 6. Images of mechanically exfoliated graphene on a SiO2/Si substrate taken by (a) AFM, (b) optical microscopy and (c) FQM using PVP/fluorescein. All scale bars = 10 μm. From Kim et al. [39]. Reprinted with permission from ACS.

Similarities between graphene and rGO are also reflected in their role as energy acceptors. However, in contrast to graphene, rGO is used most frequently as a fluorescence quencher in solutions, instead of in layer-by-layer geometries. This method, although less ordered and less controllable, may be advantageous for increasing energy/charge transfer efficiency in rGO-based assemblies. Reduced graphene oxide has been studied as an efficient fluorescence quencher of polymers [40, 41], quantum dots [42], dye-labelled aptamer [43] and also in hybrid nanostructures involving photosynthetic complexes [44]. While graphene-based hybrid structures are applied primarily for fundamental studies and to define parameters that determine energy/charge transfer, in the case of rGO composites the main focus is on potential devices and applications and optimization of their performance. Such hybrid nanostructures are considered promising for easy and relatively cheap scalable mass production of biosensors, as well as light-harvesting and optoelectronic platforms.

3. Materials and methods

In this section, we describe the structure and properties of peridinin-chlorophyll-protein (PCP), a light-harvesting pigment-protein complex, as well as graphene-based materials that are energy acceptors in our hybrid assemblies. Next, we present experimental techniques employed for investigating the energy transfer, which include—in addition to standard absorption and fluorescence spectroscopy—high-resolution confocal fluorescence microscopy coupled with time-resolved capability and spectrally resolved detection.

3.1. Peridinin-chlorophyll-protein

Peridinin-chlorophyllprotein complex from algae Dinoflagellates *Amphidinium carterae* belongs to photosynthetic complexes that are responsible for light harvesting and transfer-

ring the energy to reaction centres [2]. We focus here on aspects relevant for understanding the energy transfer between pigments comprising the PCP complex and graphene/rGO.

PCP is a water-soluble protein functioning as an antenna external to the membrane. The structure of the PCP complex, shown in **Figure 7**, has been determined with 1.3-Å resolution using X-ray crystallography [45]. In its native form, PCP consists of two chlorophyll *a* (Chl *a*) and eight peridinin (Per) molecules embedded in a protein matrix. The pigments are arranged in two almost similar clusters, with the distance between Mg atoms of the two Chl *a* in one monomer being 17.4 Å. The ratio of Per to Chl *a* of 4:1 indicates that PCP utilizes the carotenoids as its main light-harvesting pigments.

The absorption spectrum of the PCP complex, displayed in **Figure 7**, features an intense, broadband from 400 to 550 nm that is mainly due to Per absorption. The contribution of Chl *a* appears at 440 (Soret band) and 660 nm (Q_Y band). The fluorescence emission of the PCP complex originates from weakly coupled Chl molecules and it appears at 673 nm with a 30% quantum yield and a decay time constant of 4 ns, as shown by red line in **Figure 7**. Upon absorption of light, peridinins in PCP transfer their electronic excitation to Chl *a* molecules. The efficiency of this excitation energy transfer is higher than 90% as evidenced by almost ideal correspondence between absorption and fluorescence excitation spectrum. Clearly, the absorption spectrum of PCP enables the photosynthetic apparatus to harness the sunlight not only in the red spectral range but extends into the blue-green spectral region. From the point of view of the experiments described in this chapter, it is important to consider the PCP complex as a donor that can be excited at essentially any energy from 350 to 650 nm, with this excitation yielding emission at the same wavelength of 673 nm. This property distinguishes PCP, and many other photosynthetic complexes, from frequently used emitters, such as organic molecules or semiconductor quantum dots, that are much more selective in their optical characteristics.

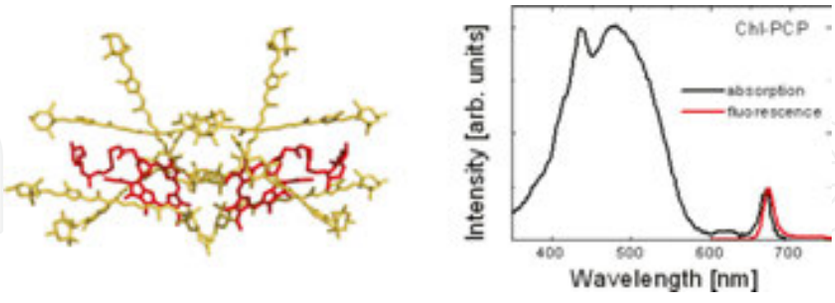

Figure 7. Pigment structure of the PCP complex together with absorption (black line) and fluorescence (red line) measured in aqueous solution at room temperature.

Previous studies of PCP complexes have been carried out on the ensemble [46, 47] and single-molecule levels [48, 49]. Transient absorption in femtosecond timescale revealed main energy transfer pathways between pigments comprising the complex, and it also was demonstrated that the interaction between the two Chl *a* molecules is relatively weak with transfer times of the order of 10 ps [47]. These findings were also corroborated with fluorescence studies of

individual PCP complexes: it has been shown that it is possible to distinguish emission originating from each of the two Chl *a* molecules and using the property of sequential photobleaching of the Chl, the energy splitting between the two molecules in the monomer was determined [49].

The simplicity of the PCP complex, its water solubility that facilitates easy sample fabrication, its small size (~4 nm) and unique spectral properties have rendered this complex as a model system for fabricating hybrid nanostructures for studying interactions at the nanoscale [3]. These include in particular extensive work focused on plasmon-induced effects associated with interactions between pigments comprising the PCP complex and metallic nanostructures [37].

3.2. Graphene-based materials

Graphene oxide was synthesized from graphite powder using the modified Hummers and Offeman method described elsewhere [50, 51]. Reduced graphene oxide was prepared from graphene oxide by reduction with hydrazine. In our procedure, graphene oxide powder (2.5 mg) was dispersed in 5 ml of distilled water and placed in an ultrasound bath for 30 min. In a separate vial, 1.55 μl of 65% hydrazine monohydrate solution was added to 1 ml of distilled water. Then, 0.5 ml of the prepared hydrazine solution was added to 0.5 mg/ml-graphene oxide solution. Finally, the mixture was transferred into a round-bottomed flask, put in an oil bath, heated up and maintained at 100°C for 24 h. After this time, a clear brown solution of graphene oxide turned into black precipitate of reduced graphene oxide flakes. The final solution was washed five times with water and ethanol, and then filtered. The remaining reduced graphene oxide flakes were dried, dissolved in distilled water and left in an ultrasound bath for 1 h before further use. As estimated from XPS measurements, *C*/*O* = 7–10 and 1.7–2 ratios were measured for rGO and GO, respectively, pointing towards substantial reduction efficiency of the synthesis procedure [52]. Afterwards, rGO flakes were dispersed in distilled water, in an ultrasound bath.

Graphene substrates were purchased from Graphene Supermarket. We used 1 × 1-cm p-doped silicon wafers with a single-layer graphene deposited using chemical vapour deposition on a 285-nm thick silicon dioxide layer. The presence of a graphene monolayer on the substrates was confirmed using Raman spectroscopy.

3.3. Sample preparation

In order to study interactions between PCP and rGO, we prepared three solutions of rGO in water, one with the initial concentration of C_0 = 0.5 mg/ml, and two dilutions, 1:10 C_0 and 1:100 C_0. To prepare the samples, we mixed PCP complexes in 2% polyvinyl alcohol (PVA) with these three rGO solutions in a 1:1 ratio. The final PCP concentration in each sample was 0.2 μg/ml. In order to compare the results obtained for the rGO-containing samples, we also prepared a reference sample, where PCP and PVA concentrations were the same as above and with rGO replaced by distilled water. The layers were obtained by spin-coating solutions on pure coverslips with the rotational speed of 1200 rpm for 2 min.

For optical experiments focused on studying excitation energy dependence of the energy transfer efficiency, we used highly diluted (optical density of 0.009 at 671 nm, concentration less than 10 μM) aqueous solution of PCP complexes. Such a low concentration is very important as on the one hand it strongly reduces the inner filter effect, but this also yields a thin layer of PCP complexes on a graphene surface. As a result, we minimize the fraction of PCP that is not coupled to graphene, thus takes no part in the energy transfer.

Finally, we fabricated structures for the evaluation of the effect of polymer layer (in our case PVA) on both interaction with graphene and photostability. To this end, samples were fabricated with the concentration of PVA varying between 0.2 and 0.002%. The obtained solutions were either drop-casted or spin-coated on single-layer graphene substrates. In the case of the latter approach, the concentration of PCP had to be adjusted to be slightly higher, as spin coating strongly reduces the number of PCP complexes within the focal volume of the focused laser.

3.4. Experimental techniques

The optical properties of hybrid nanostructures comprising light-harvesting complexes and graphene-based materials were studied using absorption and fluorescence spectroscopy in the visible spectral region. Absorption spectra were obtained using Cary 50 spectrophotometer, while fluorescence in solution was measured using Fluorolog 3 spectrofluorometer. A Xenon lamp with a double grating monochromator was used for excitation and the signal was detected with a thermoelectrically cooled photomultiplier tube characterized by a dark current of less than 100 cps.

Fluorescence intensity maps were measured with an inverted fluorescence wide-field Nikon Eclipse Ti-U microscope equipped with an Andor iXon Du-888 EMCCD detector. For each sample, a series of 50 images were acquired in order to allow for reliable statistics. Every image was collected for a different sample area, which allows for minimization of any photobleaching of the PCP fluorescence. Immersion objective with a magnification of 100× (Plan Apo, Nikon) and a numerical aperture of 1.4 was used, which provides a spatial resolution of about 300 nm. As a light source, we used LED illuminators (405, 480 and 530 nm) equipped with appropriate bandpass filters. Excitation power was equal to 50 μW. Fluorescence of PCP was extracted by combining a dichroic mirror (Chroma T650lxpr) and a bandpass filter (Thorlabs FB 670-10). Fluorescence intensity maps and kinetics were collected with the electron multiplying gain of 300× and acquisition times of 0.25 or 0.5 s, depending on the experimental conditions. White-light transmission images were recorded with the same microscope, with a halogen lamp V2-A LL (12 V, 100 W) as a light source.

Spectrally and time-resolved fluorescence measurements were performed using a home-built confocal fluorescence microscope described in detail in [53]. The sample was placed on a piezoelectric translation stage. We used pulsed laser excitation at 405, 485 and 640 nm (repetition rate of 20 MHz, average power of 30 μW, power density of ~1MW/cm^{-2}). Importantly, PCP can be efficiently excited at 405 (Soret band), at 485 (Per) and at 640 nm (excited states of chlorophylls). The laser beam was focused on the sample by LMPlan 50× objective (Olympus) with a numerical aperture of 0.5. Fluorescence was first filtered by a longpass

filter (HQ665LP Chroma) and then the spectra were detected using Andor iDus DV 420A-BV CCD camera coupled to an Amici prism. Time-resolved measurements were performed by time-correlated single-photon-counting technique using an SPC-150 module (Becker & Hickl) with fast avalanche photodiode (idQuantique id100-20) as a detector. In order to select appropriate wavelength range, we used an additional bandpass filter (FB670/10 Thorlabs). Time resolution of the TCSPC set-up is about 100 ps.

4. Results and discussion

In this section, we describe three experiments, where interactions between the PCP complexes and both rGO and epitaxial graphene were investigated. Since the PCP complexes are soluble in water, we mixed them with rGO and investigated for the energy transfer between the light-harvesting complexes and rGO. In the case of epitaxial graphene, we focus on two aspects: the dependence of the energy transfer efficiency from PCP complexes to graphene on the excitation wavelength and the influence of sample preparation on the strength of the interactions in such hybrid nanostructures.

4.1. PCP with reduced graphene oxide

Interactions between various emitters and rGO were studied so far only in solution, where ensemble averaging can smear out subtle effects associated with the interaction between emitters and rGO. Our idea was to prepare mixtures with controlled concentration of both PCP and rGO, deposit solutions on glass coverslips and image fluorescence with high spatial resolution and high sensitivity [26]. In all experiments, the concentration of PCP was maintained constant.

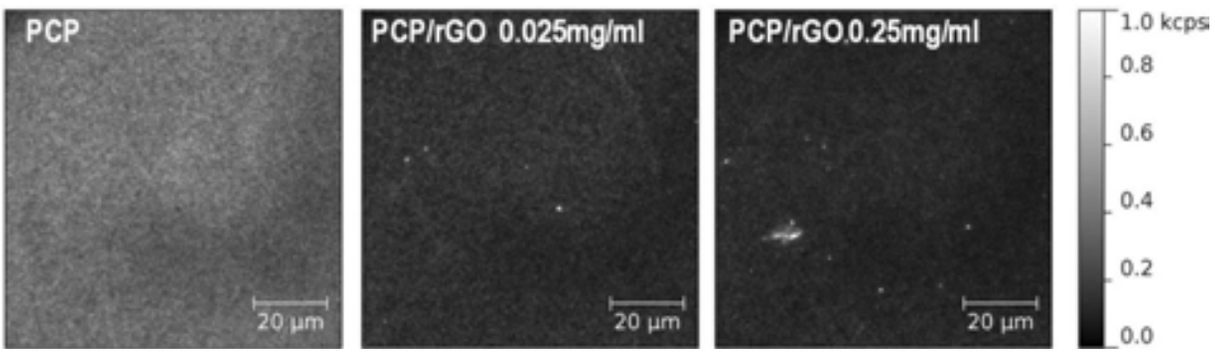

Figure 8. Fluorescence maps of (a) PCP-only reference sample and PCP/rGO mixture samples with varied rGO concentration. The excitation wavelength was 530 nm.

In **Figure 8**, we show a sequence of fluorescence maps collected for PCP complexes mixed with varied amount of rGO. The concentration of rGO was varied by orders of magnitude, so that the influence can be seen in a pronounced way. The excitation wavelength was 530 nm, but the results are qualitatively identical for the other two excitation wavelengths used in the

experiment. Incorporation of rGO induces substantial changes in fluorescence images of PCP: while for the PCP-only sample the distribution of intensity is pretty much uniform, mixing the photosynthetic complexes with rGO leads to a pattern that features high-intensity spots on an otherwise uniform background. Importantly, the intensity of these isolated bright spots is approximately 10-fold enhanced as compared to the intensity measured for the reference sample (PCP-only). At the same time, the fluorescence intensity away from the bright spots in the PCP/rGO hybrid system is quenched compared to the reference. Furthermore, the number of the bright spots increases with rGO concentration. We can exclude any contribution to this emission from GO that might be present in our sample due to non-complete reduction, as the fluorescence of GO occurs in a spectral range between 350 and 550 nm, and the emission of the PCP complexes is strongly shifted to the red. This proves that for ensemble of PCP complexes, both in the reference and in the hybrid structures (PCP/rGO) studied in this work, there is no other contribution to the measured signal.

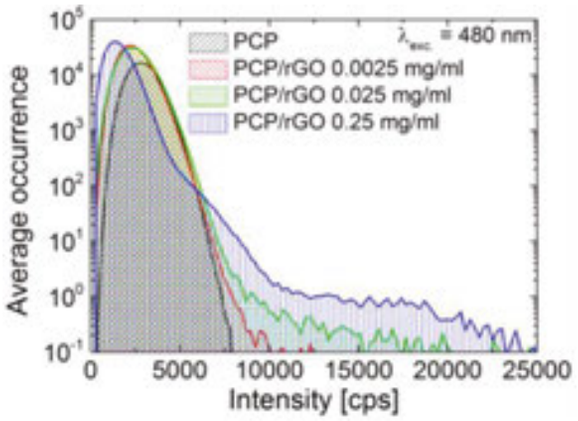

Figure 9. Histograms for PCP and PCP mixed with rGO with indicated concentrations obtained for average fluorescence intensities calculated from 50 fluorescence intensity maps for each rGO concentration. The excitation wavelength of 480 nm was used.

Statistical information about observed effects is obtained by collecting a series of more than 50 images for each sample configuration and for every excitation wavelength. In this way, we strongly reduce any possible influence of particular sample preparation or a way the experiment was carried out. Next, the fluorescence images are analysed by plotting a histogram of all the intensities measured [26]. This procedure can be applied for any single map, but also to all the maps measured for a given excitation wavelength and rGO concentration. The result of this procedure carried out of the excitation wavelength of 480 nm is displayed in **Figure 9**. The distribution of fluorescence intensity measured for the reference sample, containing only PCP complexes, features Gaussian shape, indicative of statistical distribution of concentration variation across the substrate. By contrast, the results extracted for PCP complexes mixed with rGO are more complicated. Although the majority of the intensity distribution can be approximated with Gaussian shape, similarly as in the case of the reference sample, the maximum of this distribution shifts towards lower values with increasing rGO concentration. In addition, we find considerable contribution of isolated spots spread out randomly

http://dx.doi.org/10.5772/64300

across the images, as shown in **Figure 8**, and this contribution is larger with increasing concentration of rGO in the sample. Not only the shift to lower emission intensities with incorporating rGO to the mixture as well as emergence of high-intensity spots in fluorescence images is systematic in nature, but both effects exhibit monotonic dependence on the rGO concentration in the initial solution. Indeed, for the highest rGO concentration (0.25 mg/ml), we find the largest number of bright fluorescence spots, and furthermore they exhibit the highest intensity. The results of fluorescence imaging of PCP/rGO mixtures strongly suggest that the incorporation of rGO yields both quenching of emission and formation of strongly enhanced spatially localized emitting sites. The results of fluorescence imaging show thus that the interaction between rGO and photosynthetic complexes of PCP is more complex than as discussed in a simple image of fluorescence quenching.

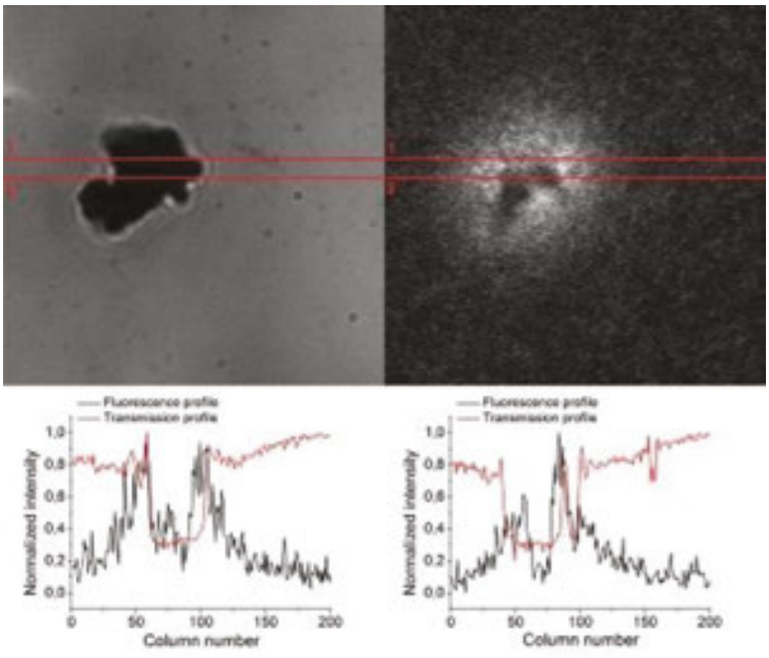

Figure 10. (Upper row) White-light transmission image of a graphene aggregate and intensity map of PCP fluorescence measured for 480-nm excitation for exactly the same location. (Lower row) Intensity profiles extracted along the cross ections marked with red lines in both images.

In order to get some insight into the possible origin of this bimodal behaviour, we also imaged a large rGO aggregate, as shown in **Figure 10**. The correspondence between transmission image and fluorescence image indicates that the same object is probed in both experiments. Even without any detailed analysis, the comparison between the two images suggests that enhanced emission occurs for PCP complexes at the edges of the flake and perhaps on its thin sections. By contrast, when the thickness of the aggregate is large, the fluorescence of PCP is efficiently quenched.

The relation between transmission and fluorescence images can be quantified using for instance Pearson correlation coefficients calculated for the two transmission-emission pair cross sections marked with red lines in **Figure 10**. For one line, we obtain a negative coeffi-

cient of −0.55, meaning that the high intensity of fluorescence correlates with dips in transmission images. A contrasting effect can be seen for the other line, where the coefficient of approximately 0.5 was obtained. Therefore, in this case, low transmission combines with quenched fluorescence. Both correlation and anti-correlation between profiles obtained for transmission and fluorescence images can be readily seen in the panels in **Figure 10**, where corresponding cross sections are plotted. These results may suggest that when a region outside the flake is considered, the correlation between emission and transmission is low. For a thin rGO flake, we find negative correlation, which could imply that PCP complexes placed at the edges of rGO experience fluorescence enhancement. Finally, for the thickest part of the flake, where both transmission and fluorescence exhibit strong decrease, the quenching is the dominant effect.

The results of fluorescence imaging of PCP/rGO hybrid nanostructures show bimodal character of the interactions. On the one hand, the fluorescence of the majority of PCP complexes is quenched; however, there are numerous localized spots characterized with considerably higher intensity. This effect depends on the rGO concentration, in particular the number of these bright spots increases with rGO concentration. While the quenching of fluorescence was observed for many graphene-based hybrid nanostructures, the enhancement is far less frequent. The exact mechanism of fluorescence enhancement is not clear, but the results show unambiguously the complexity of interactions in graphene-based photosynthetic hybrid nanostructures. Future work, which includes spectrally and temporally resolved studies, as well as experiments on large rGO flakes are in order to answer some of these questions.

4.2. Energy transfer from PCP to graphene: excitation wavelength dependence

The broad absorption of PCP complexes allows for investigating the dependence of the energy transfer efficiency on the excitation wavelength [54]. The rationale behind this experiment is that as graphene is a conductor, and contains high concentration of free carriers, it should be possible to affect the behaviour of these electrons locally using focused laser excitation. At the same time, with PCP as a donor, it is still possible to excite emission and probe the energy transfer dynamics.

In this experiment, we used epitaxial monolayer graphene transferred on 285-nm SiO_2 substrate. The optical properties of such a hybrid nanostructure were probed by time-resolved fluorescence microscopy with three excitation wavelengths of 405, 485 and 640 nm. All these wavelengths excite the emission of the PCP complexes, either via direct excitation of chlorophyll molecules or via intra-complex energy transfer from Per molecules.

In **Figure 11**, we compare fluorescence spectra measured for PCP complexes deposited on graphene with the reference. The excitation wavelength was 405 nm. This result shows substantial decrease of fluorescence intensity upon deposition of PCP on graphene, which can be tentatively attributed to the energy transfer. The decrease of fluorescence intensity is the strongest for the 405-nm excitation and the weakest for the 640-nm excitation, which again suggests that there is indeed a dependence of the energy transfer efficiency on the excitation wavelength. However, comparison of bare intensities of emission could be misleading as the

http://dx.doi.org/10.5772/64300

values might depend on many factors that can be sometimes difficult to control experimentally. However, we note that the shape of the PCP emission spectrum on graphene remains unaffected, and is identical to previously published [37], which indicates that depositing PCP on graphene leaves no measureable effect on the energy transfer pathways within the PCP complexes.

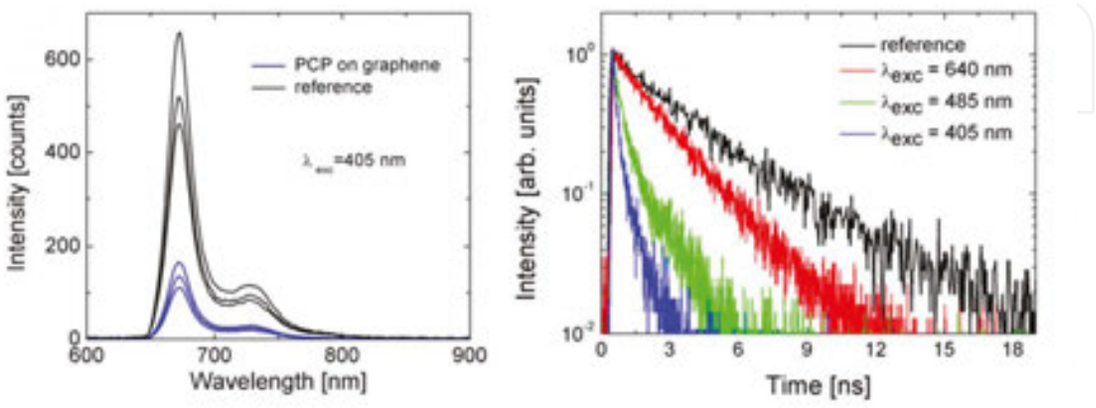

Figure 11. (Left) Fluorescence spectra of the PCP complexes deposited on graphene (blue) and on a glass substrate (black). The excitation wavelength was 405 nm. (Right) Comparison between average fluorescence transients measured for three excitation wavelengths, as indicated.

The initial assignment of the observed reduction of the emission intensity of PCP complexes deposited on graphene to the energy transfer from the chlorophylls in the photosynthetic complex to graphene is confirmed by time-resolved fluorescence spectroscopy. In **Figure 11**, we display average fluorescence transients measured for the excitation wavelengths of 405, 485 and 640 nm. The results are compared with the decay obtained for PCP complexes deposited on glass, and it has been checked that the obtained transient very weakly changes with the excitation wavelength in this case. As described in detail in [54], we find some degree of variation of fluorescence decays measured for a given excitation wavelength. It is expected, as in this experiment, that we do not control the separation between graphene and PCP complexes, and in turn introduce inhomogeneity of the interaction between the two structures across the substrate. Furthermore, it has been shown that for graphene deposited on silica, the local structure of graphene is also quite inhomogeneous with islands of high and low mobility of carriers [55]. We might therefore assume that such non-uniformity contributes to some degree to the observed spreading of fluorescence transients, although the scale of these inhomogeneities is less than 100 nm, as compared to the resolution of our microscope of about 1 μm.

Nevertheless, for both excitation wavelengths (and for 485-nm excitation as well), we observe significant shortening of fluorescence lifetime for PCP complexes deposited on graphene as compared with the reference. In addition, the 405-nm excitation yields very fast decays, while exciting with 640 nm results in considerably longer decays, regardless of the inhomogeneity of the data. It is also striking that most of them exhibit almost monoexponential behaviour, which could suggest that majority of PCP complexes within the laser spot couples to gra-

phene with a comparable strength. In no case, however, for PCP deposited on graphene we observe long (~4-ns) decay component attributable to PCP complexes isolated from graphene.

The key conclusion from these experiments is that the energy transfer to graphene depends on the excitation wavelength. Indeed, shortening of the fluorescence decay, accompanied with a decrease of the overall fluorescence intensity, observed for all used excitation wavelengths (405, 485 and 640 nm) strongly suggests that the energy absorbed by PCP complexes is efficiently dissipated into the graphene layer. Furthermore, much shorter fluorescence decay times measured for 405-nm excitation prove that the energy transfer for this excitation wavelength is more efficient compared to 640-nm excitation. The average decay times are equal to 0.5 and 1.4 ns, respectively, what translates to the energy transfer efficiencies of 87 and 65%. This is the first experimental observation of such an effect, which distinguishes graphene as a totally unique acceptor of energy in such hybrid assemblies. The qualitative picture displaying this fact is shown in **Figure 12**.

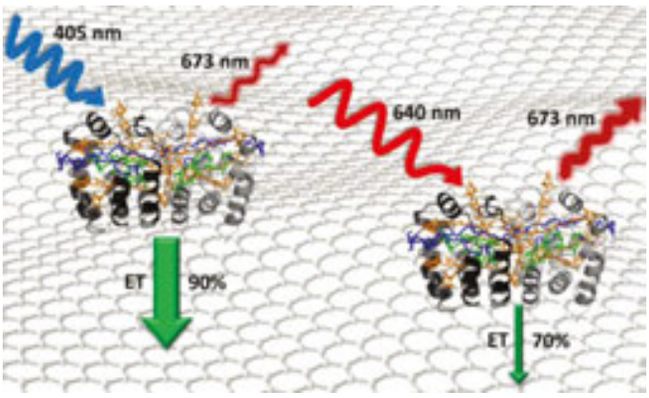

Figure 12. Schematics showing the effect of the excitation wavelength on the efficiency of the energy transfer between PCP complexes and graphene.

For molecular systems, where the energy transfer takes place between two dipole moments, the decay of a donor is independent of the excitation wavelength. This is a reminiscence of the fact that light has no effect on the surrounding of the molecules participating in the energy transfer. Apparently, for PCP complexes on graphene the situation is different. Clear influence of the excitation wavelength on the energy transfer indicates that in addition to populating PCP-excited states, laser changes also the local properties of graphene. A scenario that can explain this effect relies on the fact that focused laser excited electrons in graphene in a similar way as in metallic nanoparticle, forcing them to oscillate in a confined space defined by a monolayer of graphene on the one hand, and the size of the laser spot on the other. As a consequence, electronic excitations in chlorophylls in PCP can see graphene as a metallic nanoparticle with specific character that can influence energy dissipation.

Based on these results, we conclude that energy quenching in graphene is driven not only by dipole-dipole interaction but also by a mechanism associated with light-induced oscillations of electrons in graphene. Indeed, exciting electrons in graphene has an effect of its dissipative efficiency, which opens avenues in interfacing electronic and plasmonic character of

http://dx.doi.org/10.5772/64300

graphene in hybrid nanostructures and controls the electronic dynamics of such systems with light.

4.3. Energy transfer from PCP to graphene: influence of sample structure

An important aspect, frequently overlooked, in discussing the optical properties of hybrid nanostructures, where the interactions are distance-dependent, is the design and fabrication of layered structures. In the case of the experiment where we studied the influence of excitation energy on the efficiency of the energy transfer from PCP complexes to graphene, we used drop-casting to deposit the PCP solution on a graphene monolayer. Since it was aqueous solution, once water evaporated, PCP complexes are assumed to fall down on the graphene surface. This method, while allowing for making structures with rather well-defined geometry, results in the pigment-protein complexes being fully exposed to ambient conditions. This in turn speeds up degradation of the pigments, and the complexes as well. One of the most common ways to increase their protection against oxygen is to embed them in polymer matrix [56].

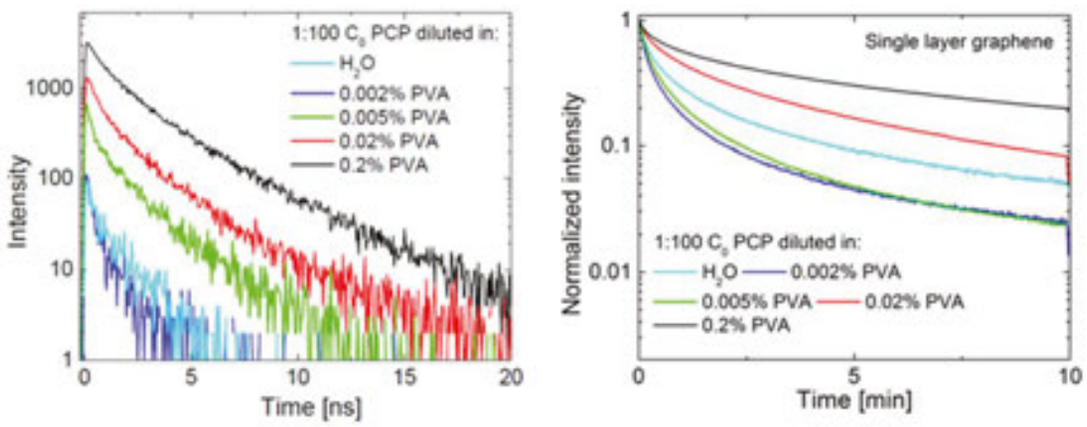

Figure 13. (Left) Fluorescence intensity decays of PCP deposited on graphene, diluted beforehand in water or in PVA aqueous solutions with varied concentrations. (Right) Corresponding kinetic curves of integrated emission intensity spectra measured in 10 min with acquisition time of 1 s. The excitation wavelength was 485 nm.

In **Figure 13**, we compare fluorescence decay curves measured for PCP complexes in water and in PVA matrix with varied concentration of the polymer, for the samples drop-casted on a single-layer graphene. The lowest concentration of PVA gives almost identical result as pure aqueous solution, in other words, the fluorescence decay is substantially shorter than the reference. This, in addition with almost monoexponential character of the decay, indicates that almost all of the PCP complexes interact with graphene, which means that the energy is transferred from chlorophylls to graphene. As the PVA concentration increases, the character of the decay changes dramatically. It is no longer monoexponential, and it features a long decay tail, reminiscent of the decay characteristic for PCP complexes that are uncoupled to graphene. This result can be understood in terms of a thicker-layer formation for a solution with higher content of PVA polymer. Such a scenario would then lead to comparatively smaller fraction of the PCP complexes that couple with graphene, most of them would be too far away from the graphene layer to experience its presence at all. This interpretation is strongly

supported by the increase of total fluorescence intensity observed with increasing concentration of PVA in solution. In fact, this increase is over an order of magnitude, although the amount of the solution deposited on a substrate is in all cases identical.

There is also another important aspect that must be considered when fabricating graphene-based hybrid nanostructures. An alternative approach to prepare layers of fluorophores on graphene substrates would be through spin coating of a solution of PCP complexes in PVA matrix. The obtained layers are much more uniform than those made by simple drop-casting, and it shows no systematic dependence on the PVA concentration. Rough estimations, based on the distribution of emission intensities measured as emission spectra or decay curves, suggest that the uniformity of the layers prepared with spin coating is about a factor of two better in terms of a standard deviation, as compared to the drop-casted samples. At the same time, the concentration of PCP complexes within the focal volume of the laser would diminish considerably as compared with the drop-casting approach; thus, this parameter must be carefully adjusted.

5. Summary and conclusions

Graphene and its derivative, reduced graphene oxide, are unique energy acceptors. While not exhibiting any fluorescence, both absorb energy in the whole visible spectral region with quite uniform efficiency. As such, graphene-based materials can be considered attractive platforms for light harvesting, energy conversion and biosensing. In this chapter, we described several experimental observations obtained for hybrid nanostructures composed of natural photosynthetic complex PCP and either graphene or reduced graphene oxide. Each studied structure sheds its own light on the mechanisms and processes that are taking place in such systems. We show that by controlling the composition of the solution and sample preparation, it is possible to tune the efficiency of the energy transfer to graphene and thus determine the sensitivity of energy transfer as a probing tool for interaction with graphene. The results obtained for PCP/rGO system indicate bimodal nature of the on-going interactions: in addition to commonly observed fluorescence quenching, we find pronounced and frequent events, where the emission of the PCP complexes is substantially enhanced. Last but not least, the uniqueness of graphene as energy acceptor manifests itself in a strong dependence of the energy transfer efficiency on the excitation wavelength. This observation allows drawing a completely new picture of the excitation dynamics, and the energy transfer, in systems where the properties of either acceptors or donors can be additionally and independently controlled by light.

Acknowledgements

This research has been supported by the WELCOME project ‘Hybrid Nanostructures as a Stepping Stone towards Efficient Artificial Photosynthesis’ funded by the Foundation for

Polish Science (FNP), by project DEC-2013/10/E/ST3/00034 from the National Science Center (NCN) and by the ORGANOMET project No: PBS2/A5/40/2014 from the National Research and Development Center (NCBiR). Izabela Kamińska acknowledges support by the Mobility Plus grant 1269/MOB/IV/2015/0 from the Polish Ministry of Science and Higher Education (MNiSW) and the START stipend awarded by the Foundation for Polish Science (FNP). We also acknowledge members of the Optics of Hybrid Nanostructures Group at the Institute of Physics, Nicolaus Copernicus University in Torun, in particular Dr. Dawid Piatkowski, Magdalena Twardowska, Justyna Grzelak, Marcin Szalkowski, and Kamil Wiwatowski for their excellent work and vital contribution.

Author details

Sebastian Mackowski[1,2*] and Izabela Kamińska[1,3]

*Address all correspondence to: mackowski@fizyka.umk.pl

1 Optics of Hybrid Nanostructures Group, Faculty of Physics, Astronomy, and Informatics, Nicolaus Copernicus University, Torun, Poland

2 Baltic Institute of Technology, BalTech, Gdynia, Poland

3 NanoBioSciences, Institute of Physical and Theoretical Chemistry, TU Braunschweig, Braunschweig, Germany

References

[1] Beljonne D, Curutchet C, Scholes, GD, Silbey RJ. Beyond Förster Resonance Energy Transfer in Biological and Nanoscale Systems. Journal of Physical Chemistry B. 2009;113:6583–6599. DOI: 10.1021/jp900708f

[2] Blankenship R. Molecular Mechanisms of Photosynthesis. Wiley-Blackwell, ISBN 978-0632-04321-7, Oxford, UK. 2008; DOI: 10.1002/9780470758472

[3] Mackowski S. Hybrid Nanostructures for Efficient Light Harvesting. Journal of Physics: Condensed Matter. 2010;22:193102/1–17. DOI:10.1088/0953-8984/22/19/193102

[4] Lakowicz J. Principles of Fluorescence Spectroscopy. 3rd edition, Springer, ISBN 978-0-387-46312-4, New York City, NY, USA. 2006; DOI: 10.1007/978-0-387-46312-4

[5] Buczynska D, Bujak L, Loi MA, Brotosudarmo THP, Cogdell R, Mackowski S. Energy Transfer from Conjugated Polymer to Bacterial Light-Harvesting Complex. Applied Physics Letters. 2012;101:173703/1–4. DOI: 10.1063/1.4764082

[6] Deng X, Tang H, Jiang J. Recent Progess in Graphene-Material-Based Optical Sensors. Analytical and Bioanalytical Chemistry. 2014;406:6903–6916. DOI: 10.1007/s00216-014-7895-4

[7] Nabiev I, Rakovich A, Sukhanova A, Lukashev E, Zagidullin V, Pachenko V, Rakovich YP, Donegan JF, Rubin AB, Govorov AO. Fluorescence Quantum Dots as Artificial Antennas for Enhanced Light Harvesting and Energy Transfer to Photosynthetic Reaction Centers. Angewandte Chemie International Edition. 2010;49: 7217–7221. DOI: 10.1002/anie.201003067

[8] Zhang J, Fu Y, Chowdhury MH, Lakowicz JR. Enhanced Förster Resonance Energy Transfer on Single Metal Particle. 2. Dependence on Donor-Acceptor Separation Distance, Particle Size, and Distance from Metal Surface. Journal of Physical Chemistry C. 2007;111:11,784–11,792. DOI: 10.1021/jp067887r

[9] Lunz M, Bradley AL, Chen WY, Gerard VA, Byrne SJ, Gun'Ko YK, Lesnyak V, Gaponik N. Influence of Quantum Dot Concentration on Förster Resonant Energy Transfer in Monodispersed Nanocrystal Quantum Dot Monolayers. Physical Review B. 2010;81:205316. DOI: 10.1103/PhysRevB.81.205316

[10] Acuna GP, Moller FM, Holzmeister P, Beater S, Lalkens B, Tinnefeld P. Fluorescence Enhancement at Docking Sites of Dna-Directed Self-Assembled Nanoantennas. Science. 2002;388:506–510. DOI: 10.1126/science.1228638

[11] Lee J, Govorov AO, Kotov NA. Bioconjugates Superstructures of CdTe Nanowires and Nanoparticles: Multistep Cascade Förster Resonance Energy Transfer and Energy Channeling. Nano Letters. 2005;5:2063–2069. DOI: 10.1021/nl051042u

[12] Geim AK, Novoselov KS. The Rise of Graphene. Nature Materials. 2007;6:183–191. DOI. 10.1038/nmat1849

[13] Novoselov KS, Fal'ko VI, Colombo L, Gellert PR, Schwab MG, Kim K. A Roadmap for Graphene. Nature. 2012;490:192–200. DOI: 10.1038/nature11458

[14] Zhu BY, Murali S, Cai W, Li X, Suk JW, Potts JR, Ruoff RS. Graphene and Graphene Oxide: Synthesis, Properties, and Applications. Advanced Materials. 2010;22:3906–3924. DOI: 10.1002/adma.201001068

[15] Castro Neto AH, Guinea F, Peres NMR, Novoselov KS, Geim AK. The Electronic Properties of Graphene. Reviews of Modern Physics. 2009;81:109–162. DOI: 10.1103/RevModPhys.81.109

[16] Nair RR, Blake P, Grigorenko AN, Novoselov KS, Booth TJ, Stauber T, Peres NMR, Geim AK. Fine Structure Constant Defines Visual Transparency of Graphene. Science. 2008;320:1308. DOI: 10.1126/science.1156965

[17] Edwards RS. Coleman KS. Graphene Synthesis: Relationship to Applications, Nanoscale. 2012;5:38–51. DOI: 10.1039/C2NR32629A

[18] Novoselov KS, Geim AK, Morozov SV, Jiang D, Katsnelson MI, Grigorieva IV, Dubonos SV, Firsov AA. Two-Dimensional Gas of Massless Dirac Fermions in Graphene. Nature. 2005;438:197–200. DOI: 10.1038/nature04233

[19] Norimatsu W, Kusunoki M. Epitaxial Graphene on SiC{0001}: Advances and Perspectives. Physical Chemistry Chemical Physics. 2013;16:3501–3511. DOI: 10.1039/C3CP54523G

[20] Zhang Y, Zhang L, Zhou C. Review of Chemical Vapor Deposition of Graphene and Related Applications. Accounts of Chemical Research. 2012;46:2329–2339. DOI: 10.1021/ar300203n

[21] Voloshina E, Dedkov Y. Graphene on Metallic Surfaces: Problems and Perspectives. Physical Chemistry Chemical Physics. 2012;12:13,502–13,514. DOI: 10.1039/C2CP42171B

[22] Hallam T, Berner NC, Yim C, Duesberg GS. Strain, Bubbles, Dirt, and Folds: A Study of Graphene Polymer-Assisted Transfer. Advanced Materials Interfaces. 2014;1:1400115/1–7. DOI: 10.1002/admi.201400115

[23] Tung VC, Allen MJ, Yang Y, Kaner RB. High-Throughput Solution Processing of Large-Scale Graphene. Nature Nanotechnology. 2009;4:25–29. DOI: 10.1038/nnano.2008.329

[24] Chua CK, Pumera M. Chemical Reduction of Graphene Oxide: A Synthetic Chemistry Viewpoint. Chemical Society Reviews. 2014;43:291–312. DOI: 10.1039/C3CS60303B

[25] Dreyer DR, Park S, Bielawski CW, Ruoff RS. The Chemistry of Graphene Oxide. Chemical Society Reviews. 2010;39:228–240. DOI: 10.1039/B917103G

[26] Twardowska M, Chomicki D, Kaminska I, Niedziołka-Jönsson J, Mackowski S. Fluorescence Imaging of Hybrid Nanostructures Composed of Natural Photosynthetic Complexes and Reduced Graphene Oxide. Nanospectroscopy. 2015;1:33–39. DOI: 10.1515/nansp-2015-0002

[27] Zhao J, Pei S, Ren W, Gao L, Cheng H.-M. Efficient Preparation of Large-Area Graphene Oxide Sheet for Transparent Conductive Films. ACS Nano. 2010;4:5245–5252. DOI: 10.1021/nn1015506

[28] Jia J, Kan C.-M, Lin X, Shen X, Kim J.-K. Effects of Processing and Material Parameters on Synthesis of Monolayer Ultralarge Graphene Oxide Sheets. Carbon. 2014;77:244–254. DOI: 10.1016/j.carbon.2014.05.027

[29] Zhou X, Liu Z. A Scalable, Solution-Phase Processing Route to Graphene Oxide and Graphene Ultralarge Sheets. Chemical Communications. 2010;46:2611–2613. DOI: 10.1039/B914412A

[30] Wang X, Bai H, Shi G. Size Fractionation of Graphene Oxide Sheets by pH-Assisted Selective Sedimentation. Journal of the American Chemical Society. 2011;133:6338–6342. DOI: 10.1021/ja200218y

[31] Lin X, Shen X, Zheng Q, Yousefi N, Ye L, Mai Y.-W, Kim J.-K. Fabrication of Highly-Aligned, Conductive, and Strong Graphene Papers Using Ultralarge Graphene Oxide Sheets. ACS Nano. 2012;6:10,708–10,719. DOI: 10.1021/nn303904z

[32] Zheng Q, Shi L, Ma P.-C, Xue Q, Li J, Tang Z, Yang, W. Structure Control of Ultra-Large Graphene Oxide Sheets by the Langmuir-Blodgett Method. RSC Advances. 2013;3:4680–4691. DOI: 10.1039/C3RA22367A

[33] Gaudreau L, Tielrooij KJ, Prawiroatmodjo GEDK, Osmond J, Garcia de Abajo FJ, Koppens FHL. Universal Distance-Scaling of Nonradiative Energy Transfer to Graphene. Nano Letters. 2013;13:2030–2035. DOI: 10.1021/nl400176b

[34] Swathi RS, Sebastian KL. Long Range Resonance Energy Transfer from a Dye Molecule to Graphene has (Distance)-4 Dependence. Journal of Chemical Physics. 2009;130:086101(1–3). DOI: 10.1063/1.3077292

[35] Berner NC, Winters S, Beckes C, Yim C, Dümbgen KC, Kaminska I, Mackowski S, Cafolla AA, Hirsch A, Duesberg GS. Understanding and Optimizing the Packing Density of Perylene Bisimide Layers on CVD-Grown Graphene. Nanoscale. 2015;7:16,337–16,342. DOI: 10.1039/C5NR04772B

[36] Chen Z, Berciaud S, Nuckolls C, Heinz TF, Brus LE. Energy Transfer from Individual Semiconductor Nanocrystals to Graphene. ACS Nano. 2010;4:2964–2968. DOI: 10.1021/nn1005107

[37] Mackowski S., Metallic Nanoparticles Coupled to Photosynthetic Complexes, Smart Nanoparticles Technology , ISBN 978-953-51-0500-8, ed. A. Hashim, InTech Publishing, 2012, 3–28; DOI: 10.5772/33493

[38] Federspiel F, Froehlicher G, Nasilowski M, Pedetti S, Mahmood A, Doudin B, Park S, Lee J.-O, Halley D, Dubertret B, Gilliot P, Berciaud S. Distance Dependence of the Energy Transfer Rate from a Single Semiconductor Nanostructure to Graphene. Nano Letters. 2015;15:1252–1258. DOI: 10.1021/nl5044192

[39] Kim J, Cote LJ, Kim F, Huang J. Visualizing Graphene Based Sheets by Fluorescence Quenching Microscopy. Journal of the American Chemical Society. 2010;132:260–267. DOI: 10.1021/ja906730d

[40] Wang Y, Kurunthu D, Scott GW, Bardeen CJ. Fluorescence Quenching in Conjugated Polymers Blended with Reduced Graphene Oxide. Journal of Physical Chemistry C. 2010;114:4153–4159. DOI: 10.1021/jp9097793

[41] Ran C, Wang M, Gao W, Ding J, Shi Y, Song X, Chen H, Ren Z. Study of Photoluminescence Quenching and Photostability Enhancement of MEH-PPV by Reduced Graphene Oxide. Journal of Physical Chemistry C. 2012;116:23,053–23,060. DOI: 10.1021/jp306631y

[42] Samal M, Mohapatra P, Subbiah R, Lee C.-L, Annas B, Kim JA, Kim T, Yi DK. InP/ZnS-graphene Oxide and Reduced Graphene Oxide Nanocomposites as Fascinating

Materials for Potential Optoelectronic Applications. Nanoscale. 2013;5:9793–9805. DOI: 10.1039/C3NR02333H

[43] Zhao H, Gao S, Liu M, Chang Y, Fan X, Quan X. Fluorescent Assay for Oxytetracycline based on a Long-Chain Aptamer Assembled onto Reduced Graphene Oxide. Microchimica Acta. 2013;180:829–835. DOI: 10.1007/s00604-013-1006-7

[44] Twardowska M, Kamińska I, Wiwatowski K, Ashraf KU, Cogdell RJ, Mackowski S, Niedziółka-Jönsson J. Fluorescence Enhancement of Photosynthetic Complexes Separated from Nanoparticles by a Reduced Graphene Oxide Layer. Applied Physics Letters. 2014;104:093103/1–5. DOI: 10.1063/1.4867167

[45] Hofmann E, Wrench P, Sharples F, Hiller R, Welte W, Diederichs K. Structural Basis of Light Harvesting by Carotenoids: Peridinin-Chlorophyll-Protein from *Amphidinium carterae*. Science. 1996;272:1788–1791. DOI: 10.1126/science.272.5269.1788

[46] Akimoto S, Takaichi S, Ogata T, Nishimura Y, Yamazaki I, Mimuro M. Excitation Energy Transfer in Carotenoid Chlorophyll Protein Complexes Probed by Femtosecond Fluorescence Decays. Chemical Physics Letters. 1996;260:147–152. DOI: 10.1016/0009-2614(96)00863-9

[47] Kleima F, Hofmann E, Gobets B, van Stokkum I, van Grondelle R, Diederich K, van Amerongen H. Förster Excitation Energy Transfer in Peridinin-Chlorophyll a-Protein. Biophysical Journal. 2000;78:344–353. DOI: 10.1016/S0006-3495(00)76597-0

[48] Mackowski S, Wörmke S, Brotosudarmo T, Jung C, Hiller R, Scheer H, Bräuchle C. Energy Transfer in Reconstituted Peridinin-Chlorophyll-Protein Complexes: Ensemble and Single Molecule Spectroscopy Studies. Biophysical Journal. 2007;93:3249–3258. DOI: 10.1529/biophysj.107.112094

[49] Wörmke S, Mackowski S, Jung C, Ehrl M, Zumbusch A, Brotosudarmo T, Scheer H, Hofmann E, Hiller R, Bräuchle C. Monitoring Fluorescence of Individual Chromophores in Peridinin-Chlorophyll-Protein Complex Using Single Molecule Spectroscopy. Biochimica et Biophysica Acta – Bioenergetics. 2007;1767:956–964. DOI: 10.1016/j.bbabio.2007.05.004

[50] Pei S, Cheng H.-M. The Reduction of Graphene Oxide. Carbon. 2012;50:1972–2012. DOI: 10.1016/j.carbon.2011.11.010

[51] Mao S, Pu H, Chen J. Graphene Oxide and its Reduction: Modeling and Experimental Progress. RSC Advances. 2012;2:2643–2662. DOI:10.1039/C2RA00663D

[52] Kaminska, I, Barras A, Coffinier Y, Lisowski W, Niedziołka-Jönsson J, Woisel P, Lyskawa J, Opallo M, Siriwardena A, Boukherroub R, Szunerits S. Preparation of a Responsive Carbohydrate-Coated Biointerface based on Graphene/Azido-Terminated Tetrathiafulvalene Nanohybrid Material. ACS Applied Materials & Interfaces. 2012;4:5386–5393. DOI: 10.1021/am3013196

[53] Krajnik B, Schulte T, Piatkowski D, Czechowski N, Hofmann E, Mackowski S. SIL-based Confocal Fluorescence Microscope for Investigating Individual Nanostruc-

tures. Central European Journal of Physics. 2011;9:293–299. DOI: 10.2478/s11534-010-0098-5

[54] Mackowski S, Kaminska, I. Dependence of the Energy Transfer to Graphene on the Excitation Energy. Applied Physics Letters. 2015;107:023110/1–4. DOI: 10.1063/1.4926984

[55] Burson KM, Cullen WG, Adam S, Dean CR, Watanabe K, Taniguchi T, Kim P, Fuhrer MS. Direct Imaging of Charged Impurity Density in Common Graphene Substrates. Nano Letters. 2013;13:3576–3580. DOI: 10.1021/nl4012529

[56] Wörmke S, Mackowski S, Schaller A, Brotosudarmo T, Johanning S, Scheer H, Bräuchle C. Single Molecule Fluorescence of Native and Refolded Peridinin-Chlorophyll-Protein Complexes. Journal of Fluorescence. 2008;18:611–617. DOI: 10.1007/s10895-008-0310-9